Original Article

Structural Insight into Anaphase Promoting Complex 3 Structure and Docking with a Natural Inhibitory Compound

Hamzeh Rahimi, Mohammad Ali Shokrgozar[1], Armin Madadkar-Sobhani[2,3], Reza Mahdian, Alireza Foroumadi[4], Morteza Karimipoor

From the Department of Molecular Medicine, Biotechnology Research Center, [1]National Cell Bank of Iran, Pasteur Institute of Iran, Tehran, [2]Department of Life Sciences, Barcelona Supercomputing Center, Barcelona, Spain, [3]Department of Bioinformatics, Institute of Biophysics and Biochemistry, University of Tehran, [4]Department of Medicinal Chemistry, Faculty of Pharmacy and Pharmaceutical Sciences Research Center, Tehran University of Medical Sciences, Tehran, Iran

Address for correspondence:
Dr. Morteza Karimipoor, Department of Molecular Medicine, Biotechnology Research Center, Pasteur Institute of Iran, PO Box: 1316943551, Tehran, Iran.
E-mail: mortezakarimi@yahoo.com

Abstract

Background: Anaphase promoting complex (APC) is the biggest Cullin-RING E3 ligase and is very important in cell cycle control; many anti-cancer agents target this. APC controls the onset of chromosome separation and mitotic exit through securin and cyclin B degradation, respectively. Its APC3 subunit identifies the APC activators-Cdh1 and Cdc20. **Materials and Methods:** The structural model of the APC3 subunit of APC was developed by means of computational techniques; the binding of a natural inhibitory compound to APC3 was also investigated. **Results:** It was found that APC3 structure consists of numerous helices organized in anti-parallel and the overall model is superhelical of tetratrico-peptide repeat (TPR) domains. Furthermore, binding pocket of the natural inhibitory compound as APC3 inhibitor was shown. **Conclusion:** The findings are beneficial to understand the mechanism of the APC activation and design inhibitory compounds.

Keywords: *Anaphase promoting complex, bioinformatics, tetratrico-peptide repeat domain*

Introduction

Many proteins regulate the cell cycle and progression through the cell cycle is dependent on their sequential degradation,[1] which is carried out by the anaphase promoting complex (APC) and the SKP1-CUL1-F-boxprotein (SCF).[2] APC contains two active shapes: APC^{Cdc20}, which is active over the M-step of the cell cycle and APC^{Cdh1}, which controls mitotic exit and the G1 step.[2] APC controls the metaphase-anaphase transition, mitotic exit, and G1 progression through mediating, respectively, securin and cyclin degradation.[3] So as to develop the metaphase-anaphase transition, APC^{Cdc20} adds various ubiquitin molecules to securin in the M phase. Separase is activated after securin degradation, resulting in cohesion cleavage, chromosome segregation and, ultimately, cell entrances into the anaphase.[4] At the final phase of the mitotic exit, cytokinesis, APC acts as a regulating agent by means of targeting aurora kinase.[5] Moreover, the cell cycle is correlated with other pathways by pathways by APC, e.g., the chromosome segregation,[6] transcription,[7] Deoxyribose Nucleic Acid (DNA) replication,[8] transforming growth factor beta (TGF-β) signaling, and glycolysis pathways[9] to ensure cell growth and division at the right time. APC also controls the mitochondrial function through selective protein degradation to prepare the energy required over the cell cycle progression.[10]

An enzymatic cascade including the ubiquitin-activating enzyme (E1), ubiquitin conjugating enzymes (E2s) and E3 ligase enzymes happen in the ubiquitination reaction.[11] First, the ubiquitin is attached to the last residue G76, which is a thioester linkage with the cysteine residue in the active site of ubiquitin-activating enzyme (E1). Next, it is transferred from E1 to the cysteine residue in the active site of the E2, needing hydrolysis of ATP. Under physiological situations, UbcH10 and UbcH5 act as E2 enzymes for APC,[12-13] whereas the E3 ligase acts as the scaffold for the ubiquitination reaction. The E3 ligase is bound to the E2 and the substrate simultaneously and the transfer of the ubiquitin from UbcH10 to a lysine residue on the substrate[14] is done easier. Finally, the poly-ubiquitinated substrates degradation happens by the 26S proteasome.[15]

The activation of APC happens through binding by two co-activators: Cdh1 and

How to cite this article: Rahimi H, Shokrgozar MA, Madadkar-Sobhani A, Mahdian R, Foroumadi A, Karimipoor M. Structural Insight into Anaphase Promoting Complex 3 Structure and Docking with a Natural Inhibitory Compound. Adv Biomed Res 2017;6:26.

Received: March, 2013. **Accepted:** May, 2013.

Access this article online

Website: www.advbiores.net

DOI: 10.4103/2277-9175.201683

Quick Response Code:

Cdc20, and phosphorylation on various subunits.[16] A vast spectrum of substrates via their destruction box and KEN (Lys-Glu-Asn) motif can be recognized by the co-activators.[17] APC is inhibited by the early mitotic inhibitor-1 (*Emi1*), mitotic checkpoint complexes (including Mad2, Bub3, BubR1/Mad3, and Cdc20) and RASSF1A in the S, G2, and prometaphase steps.[18-19]

APC, which has 13 subunits, is the most complex representative of the RING/cullin family of multi-subunit E3 ligases.[20] Its subunits are located in three sub-complexes: I. the catalytic sub-complex (Doc1/APC10, APC11, and APC2), II. A structural or scaffold sub-complex (APC1, APC4, and APC5), and III. A tetratrico-peptide repeat (TPR) sub-complex (APC3/6/7/8/13).[21] The function of tetratrico-peptide repeat (TPR) subunits is binding to the co-activators (Cdh1 and Cdc20) and enhancing the self-assembly of the complex.[22] The scaffold sub-complex is comprised of the largest subunits like APC1 (1,944 residues), and prepares the platform for substrate recognition and reaction catalysis through the other sub-complexes.[23]

The first time TRP motif was discovered in APC subunits.[20,24-27] This motif is also found in the N-terminal region of BubR1,[28] Hsp90,[29] the nicotinamide adenine dinucleotide phosphate (NADPH) oxidase subunit *p67phox*,[30] Hsp90-binding immunophilins,[31] and transcription factors.[32] Each TPR motif has 34 degenerative residues which make a helix-turn-helix structure.[33] TPRs are placed in a parallel arrangement. APC3 containing 822 residues is a critical subunit of APC for binding to Cdh1 or Cdc20 and play a role as linker between catalytic sub-complex and TPR subunits in TRP sub-complex of APC.[4,34] It was shown that APC3 is bound to Microcephalin (*MCPH1*), which is causative for main recessive autosomal microcephaly.[35]

Despite the fact that there is much information regarding APC function in different conditions and cell cycle phases, the structure of APC is still unknown. This is, in part, due to the fact that there are many technical problems in the expression of complicated protein complexes such as APC. In addition, such protein complexes still are assembled and crystallized difficultly. Thus, in this study, a 3D structural model of APC3 was developed and the binding of tosyl-L-arginine methyl ester (TAME), as an inhibitory compound with APC3 subunit, was investigated using full flexible docking algorithms to elucidate the TAME binding pocket on the APC3. TAME, known as APC inhibitor, inhibits APC function via competition with Inverted Repeat motif of Cdc20 and Cdh1, APC co-activators. The effective concentration of TAME for APC inhibition *in vitro* is 12 μM.[36] It is recommended that tosyl, arginine groups of TAME are involved in receptor binding. The results prepare a structural viewpoint of the model of APC3. The binding pocket, which is crucial to design new inhibitory compounds, was identified.

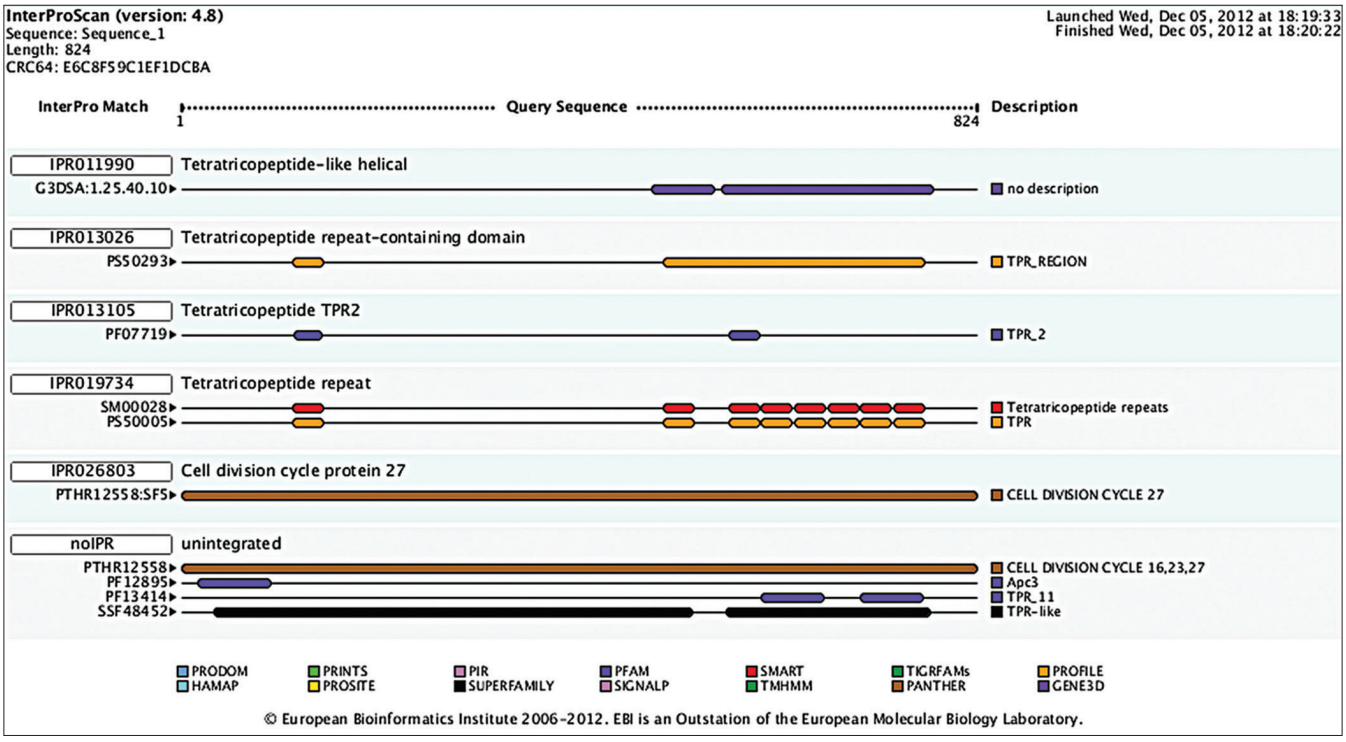

Figure 1: APC3 domain distribution. TPR domains are located in N-terminal and C-terminal regions. Although just one repeat was seen in N-terminal region, other repeats are arranged in tandem in C-terminal region

Materials and Methods

Multiple sequence alignment and homology modeling

In order to find homologous sequences, the UniProt database was applied.[37] After the fragmented and unrelated sequences were removed, repossessed sequences were introduced to ClustalW[38] for multiple sequence alignment using Clustal algorithm, BLOSUM62 scoring matrix and default parameter settings. The JalView software[39] was used to visualize the results of the alignment. Secondary structure patterns were projected through Jpred.[40]

So as to perform homology modeling, the MODELLER 9.10 package[41] was used. Sequence-structure alignment against Protein Data Bank (PDB) database was conducted by means of HHpred toolkit[42] to find a homologous structure as a template for homology modeling (HM). For APC3 modeling, 10,000 models were produced and the best model was chosen in accordance with Discrete Optimized Protein Energy (DOPE) score.

Molecular dynamics

Energy minimization was carried out for the models of the APC3 subunit by using molecular dynamic (MD) simulations in Gromacs 4.5 software[43] with Amber99SB-ILDN force field[44] and TIP3P explicit waters.[45] 0.15 M Na^+ and Cl^- were added to the water box to neutralize the system for simulation of the physiological environment. In order to provide the system, energy minimization was initiated by using a steepest-descent algorithm with a tolerance of 10 kJ/mol/nm and a 2 fs step size. Hydrogen atoms were allowed to be relaxed with fixed heavy atoms for 50 ps with a step size of 2 fs during the position-restraining step. All bonds were restrained through the linear constraint solver (LINCS) algorithm.[46] There were two steps in system equilibration: Firstly, the system was heated for 100 ps by means of V-rescale algorithm for temperature stabilization (T = 300 K with temperature coupling τP = 0.1 ps).[47] Next, the pressure coupling was run for 50 ps using the Parrinello-Rahman method in order to stabilize pressure (P = 1, τP = 0.1 ps).[48] For the calculation of electrostatics and van der Waals (VDW) interactions with grid spacing of 0.16 nm and 1.4 nm as cut off, the smooth Particle Mesh Ewald method was employed.[49] Finally, the MD simulation was done with a time step of 2.0 fs for 10 ns.

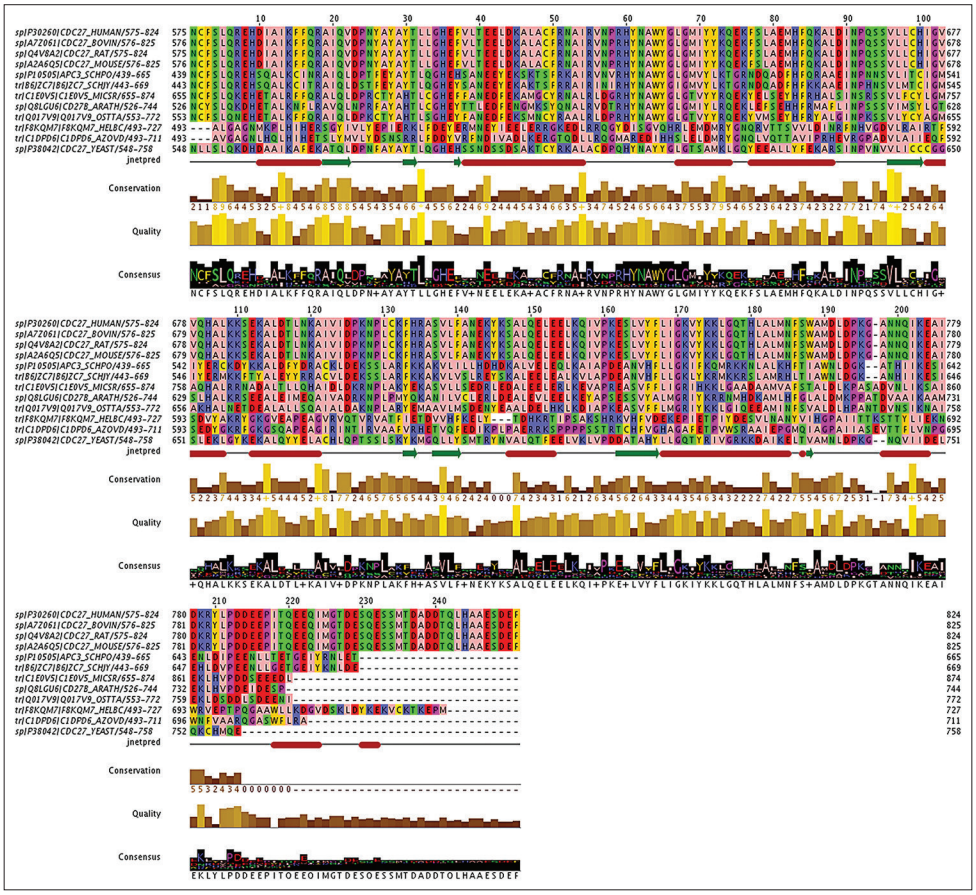

Figure 2: Multiple sequence alignment of C-terminal region APC3. Sequence alignment shows conservation in C-terminal region. Secondary structure prediction was performed by JPred software. Most of regions were predicted as α-helix region. Alignment includes APC3 sequence from the following organisms: sp | P30260 | CDC27_HUMAN, sp | A7Z061 | CDC27_BOVIN, sp | Q4V8A2 | CDC27_RAT, sp | A2A6Q5 | CDC27_MOUSE, sp | P10505 | APC3_SCHPO, tr | B6JZC7 | B6JZC7_SCHJY, tr | C1E0V5 | C1E0V5_MICSR, sp | Q8LGU6 | CD27B_ARATH, tr | Q017V9 | Q017V9_OSTTA, tr | F8KQM7 | F8KQM7_HELBC, tr | C1DPD6 | C1DPD6_AZOVD and sp | P38042 | CDC27_YEAST

Analysis of the molecular dynamic simulations

To analyse and visualize the result of the APC3 simulation, Gromacs 4.5 and PyMol softwares were used. For each trajectory, energy analysis including temperature, pressure, potential energy, and kinetic energy was conducted. Root mean square deviation (RMSD) between the starting structure and the average structure was applied to study the structural convergence. Protein stability and flexibility was controlled by means of root mean square fluctuation (RMSF) and secondary structure analysis. The average structure was extracted from trajectory between 3,000 and 10,000 frames (steps) and then energy was minimized by steepest-descent and the conjugate-gradients method. The structure validation was performed by torsion angles analysis of the protein backbone (*phi* and *psi*) through PROCHECK software,[50] Z-scor, Verify3D, prosaII score, Molprobity.[51]

Molecular docking

Ligand and receptor preparation involve add Hydrogen, charge and miss-atom was carried out using ADT4.2 toolkit.[52] Interacting residue diagram was drawn using LigPlot + software.[53]

Results

Architecture of the anaphase promoting complex 3

In APC3 sequence, eight TPR domains were found in the 115-148 and C-terminal regions (499-770) using InterProScan and Prosite [Figure 1]. Conservation in C-terminal region (580-822) was shown in multiple sequence alignment of APC3 from different organisms [Figure 2].

Anaphase-promoting complex subunit CUT9 (PDB ID: 2XPI) was selected as the template for APC3 structure prediction based on the structure-sequence alignment. This protein is related to *Schizosaccharomyces pombe* and contains TPR domains. Because of the high resolution (2.06 A°) and the presence of TPR domain, the CUT9 is a suitable template for HM. Homology was shown from the middle to end of APC3 (260-822) in the structure-sequence alignment. To select the best model based on DOPE score, 10,000 models were generated by means of MODELLER. The best structural model contains many α-helices localized in anti-parallel [Figure 3a]. Each TPR domain contains two α-helices (A and B) that are connected to each other via a turn region [Figure 3b]. Adjacent TPR domains were bound via a long loop. Each loop has internal curve that accelerates the interaction among close TPR domains. In the N-terminal, six TPR domains form a circle around the central axis. The outside of the circle is made up of β helix from each TPR domain and α helix is localized in the internal side [Figure 3b]. Other TPR domains are placed in the second circle. These circles are bound to each other via the seventh TPR domain tending toward the C-terminal region. The α-helix of the last TPR domain has an unstructured region. From the top view, the overall structure is superhelix, similar to the regular helices that were seen in a solenoid shape [Figure 3b]. MD simulation was performed for 10 nano-seconds to reveal the structural stability of structural model. RMSF plot was shown that the structural model is stable during the MD simulation [Figure S1] except for some residues in C-terminal. It was found that all of residues are in allowed region as shown in the Ramachandran plot [Figure 4b]. Moreover, superposition of the average and B-factor structures [Figure 4a] indicates high stability in the all regions, apart from the last TPR domain.

Molecular docking

In this study, molecular docking was used to investigate the binding of TAME to APC3. ADT4.2 toolkit and vina-autodock were applied to dock; the LigPlot software was used for visualization of the binding pocket. It was found that TAME was bound to APC3 with high affinity (−6.2 kcal/mol) [Figure 5a-c]. The docking environment was set up to cluster the different structural conformations into nine classes. As can be seen in Table 1, binding affinity of the different classes is very near each other (from −5.4 to −6.2). Furthermore, it was found that all classes were bound to a same binding pocket [Figure 5d], except for class 7, which had much conformational change (RMSD = 20.672) and was bound to another lactation on APC3 [Figure 5d]. Representation of the LigPlot result was shown that binding pocket was

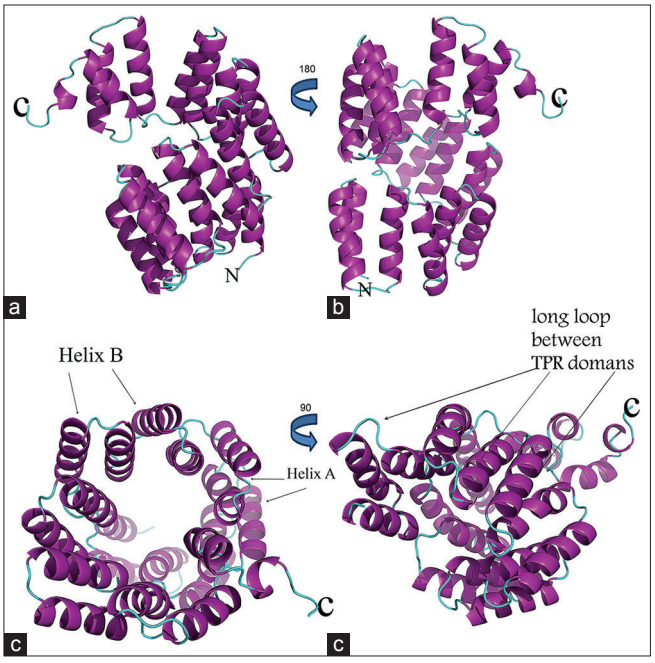

Figure 3: Three dimensional structure of human APC3. (a and b) The front view of APC3 structure that contain TPR domains. (c and d) The top view of APC3, which is similar to super-helix. Purple color represents helix and cyan color shows loop region. All panels were prepared by PyMOL software (www.PyMOL.org)

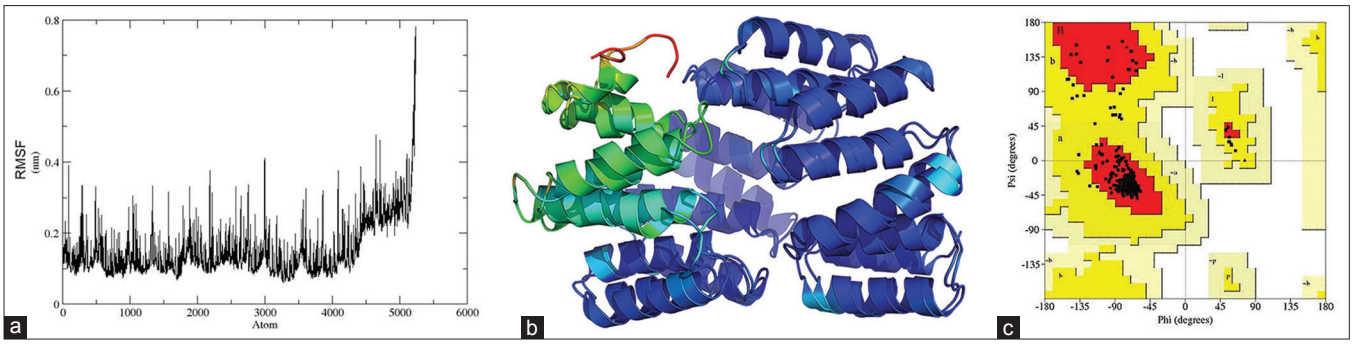

Figure 4: APC3 structure validation. (a) RMSF (root mean square fluctuation) showed that the APC3 structure model is stable during MD, only the last TPR domain has more flexibility. (b) Superposition of the average and B-factor structures, red color showed more flexible region and blue color represent the stable region. Here, only the last TPR domain has conformational changes. (c) In Ramachandran plot, 91% residues were in most favored regions and the other residues (8.9%) put in allowed additional region

Table 1: Binding affanity of diffrent conformational structures of TAME to APC3

Class	Affinity (kcal/mol)	Distance from best mode (RMSD)
1	–6.2	0.000
2	–5.9	3.168
3	–5.8	2.285
4	–5.8	2.530
5	–5.7	2.103
6	–5.5	3.177
7	–5.5	20.672
8	–5.4	2.326
9	–5.4	2.914

RMSD: Root mean square deviation, TAME: Tosyl-L-arginine methyl ester

comprised of 12 residues; four of which (*Val179, Tyr148, Glu291*, and *Lys247*) involve in the hydrogen bond. Eight non-hydrogen (van der waals) bonds were also seen in the binding pocket [Figure 6].

Discussion

Anaphase promoting complex 3 structure

APC, is a prominent member of the cullin-RING E3 ligase family, includes both cullin and RING domains in the catalytic subunits.[54] TPR domains are seen in proteins with different functions such as synaptosomal-associated protein (SNAP) secretary proteins, N-terminal region of BubR1,[28] Hsp90,[29] APC subunits Cdc16, Cdc23, and Cdc27,[20,24-27] the NADPH oxidase subunit *p67phox*,[30] Hsp90-binding immunophilins,[31] and transcription factors.[32] The TPR domain plays a role in complex assembly,[55] cytoplasmic accumulation[56] and it is considered as ligand (peptide) in domain binding[57]; a number of TPR domains are important in protein-protein interaction.[58] In APC3, the TPR domains were bound to Cdh1 and accelerate APC activation.[34] In this work, the structural model of APC3 was developed and the binding of the natural inhibitory compound (TAME) to APC3 was studied. It was found that APC3 had eight TPR domains

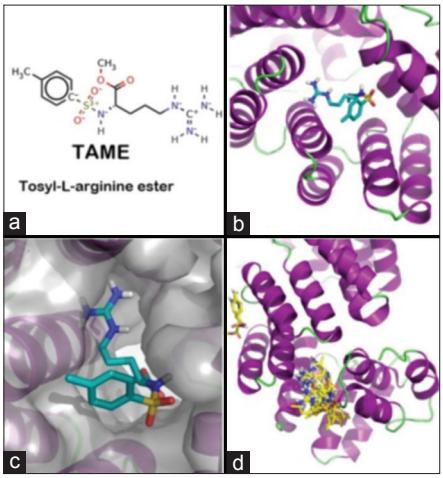

Figure 5: TAME binding to APC3. (a) Two dimentional representation of TAME. (b and c) Binding pocket of TAME, which is located in TPR repeats. (d) Orentation of different conformational clusters of TAME showed that all of them are localized in same binding pocket expet for the seventh cluster

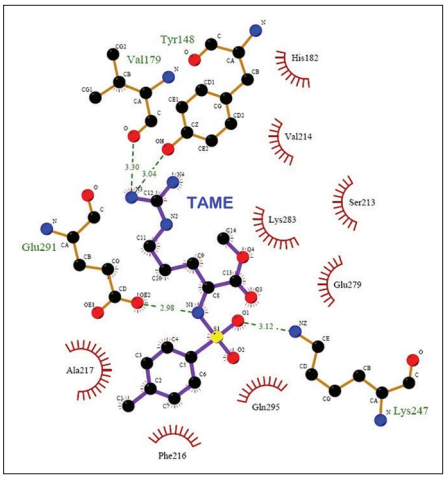

Figure 6: TAME binding pocket. This binding pocket is composed of 12 residues in which four of them involve in hydrogen bond (*Val179*, *Tyr148*, *Glu291*, and *Lys247*)

in the central and C-terminal region. The overall structure of APC3 is solenoid shaped [Figure 3]. Structural analysis of Protein phosphatase 5 (PP5) containing TPR domains

revealed that the TPR motif is a pair of anti-parallel α-helices associated together with a packing angle of ~ 24° between helix axes.[59] APC3 has a structural conformation change in C-terminal [Figures 4a and b], which helps to Cdh1 recognition because this structure is very compact, and provides enough space to interact with Cdh1. Such conformational change is found in other Cdh1 recognition proteins such as APC10,[60-62] which makes an activator recognition site in association with APC3.

Tosyl-L-arginine methyl ester molecular docking

TAME is a natural small molecule extracted from *Xenopus* extract. Previous studies showed that TAME is bound to APC3 and inhibits APC complex activity.[36] Many of researchers reported that C-terminal region of APC3 (499-824) has a role in binding to co-activators and APC inhibitors (TAME and pseudosubstrate).[36,63] In the present study, it was found that TAME is bound to APC3 in high affinity; the binding pocket is located in TPR domains. This binding may result in arresting in domain movement which inhibits APC function. This hypothesis is confirmed by a study on binding of peptide to the TPR domai[63] that showed binding of peptide to TPR domain increased structure rigidity. Therefore, the TPR domain couldn't associate with other proteins. Moreover, TAME was bound to the TPR domain in the C-terminal region, where play a role in binding to Cdh1. Based on docking pattern, similarity search methods were used in small molecules database to find molecules with high affinity and low toxicity.

Acknowledgment

This work was funded by PhD student grant from Pasteur Institute of Iran.

Financial support and sponsorship

This work was funded by PhD student grant from Pasteur Institute of Iran.

Conflicts of interest

There are no conflicts of interest.

References

1. Rape M, Kirschner MW. Autonomous regulation of the anaphase-promoting complex couples mitosis to S-phase entry. Nature 2004;432:588-95.
2. Mocciaro A, Rape M. Emerging regulatory mechanisms in ubiquitin-dependent cell cycle control. J Cell Sci 2012;125(Pt 2):255-63.
3. Cooper KF, Strich R. Meiotic control of the APC/C: Similarities and differences from mitosis. Cell Div 2011;6:16.
4. Izawa D, Pines J. How APC/C-Cdc20 changes its substrate specificity in mitosis. Nat Cell Biol 2011;13:223-33.
5. Floyd S, Pines J, Lindon C. APC/C Cdh1 targets aurora kinase to control reorganization of the mitotic spindle at anaphase. Current Biol 2008;18:1649-58.
6. Reddy SK, Rape M, Margansky WA, Kirschner MW. Ubiquitination by the anaphase-promoting complex drives spindle checkpoint inactivation. Nature 2007;446:921-5.
7. Turnell AS, Stewart GS, Grand RJ, Rookes SM, Martin A, Yamano H, *et al.* The APC/C and CBP/p300 cooperate to regulate transcription and cell-cycle progression. Nature 2005;438:690-5.
8. Mailand N, Diffley JF. CDKs promote DNA replication origin licensing in human cells by protecting Cdc6 from APC/C-dependent proteolysis. Cell 2005;122:915-26.
9. De Boeck M, ten Dijke P. Key role for ubiquitin protein modification in TGFbeta signal transduction. Ups J Med Sci 2012;117:153-65.
10. Garedew A, Andreassi C, Moncada S. Mitochondrial dynamics, biogenesis, and function are coordinated with the cell cycle by APC/C CDH1. Cell Metab 2012;15:466-79.
11. Meyer HJ, Rape M. Processive ubiquitin chain formation by the anaphase-promoting complex. Semin Cell Dev Biol 2011;22:544-50.
12. Rape M, Reddy SK, Kirschner MW. The processivity of multiubiquitination by the APC determines the order of substrate degradation. Cell 2006;124:89-103.
13. Mathe E, Kraft C, Giet R, Deak P, Peters JM, Glover DM. The E2-C vihar is required for the correct spatiotemporal proteolysis of cyclin B and itself undergoes cyclical degradation. Curr Biol 2004;14:1723-33.
14. Wu T, Merbl Y, Huo Y, Gallop JL, Tzur A, Kirschner MW. UBE2S drives elongation of K11-linked ubiquitin chains by the anaphase-promoting complex. Proc Natl Acad Sci U S A 2010;107:1355-60.
15. Min M, Lindon C. Substrate targeting by the ubiquitin-proteasome system in mitosis. Semin Cell Dev Biol 2012;23:482-91.
16. Kraft C, Herzog F, Gieffers C, Mechtler K, Hagting A, Pines J, *et al.* Mitotic regulation of the human anaphase-promoting complex by phosphorylation. EMBO J 2003;22:6598-609.
17. Thornton BR, Toczyski DP. Precise destruction: An emerging picture of the APC. Genes Dev 2006;20:3069-78.
18. Ban KH, Torres JZ, Miller JJ, Mikhailov A, Nachury MV, Tung JJ, *et al.* The END network couples spindle pole assembly to inhibition of the anaphase-promoting complex/cyclosome in early mitosis. Dev Cell 2007;13:29-42.
19. Song MS, Song SJ, Ayad NG, Chang JS, Lee JH, Hong HK, *et al.* The tumour suppressor RASSF1A regulates mitosis by inhibiting the APC-Cdc20 complex. Nat Cell Biol 2004;6:129-37.
20. Thornton BR, Ng TM, Matyskiela ME, Carroll CW, Morgan DO, Toczyski DP. An architectural map of the anaphase-promoting complex. Genes Dev 2006;20:449-60.
21. Schreiber A, Stengel F, Zhang Z, Enchev RI, Kong EH, Morris EP, *et al.* Structural basis for the subunit assembly of the anaphase-promoting complex. Nature 2011;470:227-32.
22. Matyskiela ME, Morgan DO. Analysis of activator-binding sites on the APC/C supports a cooperative substrate-binding mechanism. Mol Cell 2009;34:68-80.
23. Herzog F, Primorac I, Dube P, Lenart P, Sander B, Mechtler K, *et al.* Structure of the anaphase-promoting complex/cyclosome interacting with a mitotic checkpoint complex. Science 2009;323:1477-81.
24. Wang J, Dye BT, Rajashankar KR, Kurinov I, Schulman BA. Insights into anaphase promoting complex TPR subdomain assembly from a CDC26-APC6 structure. Nat Struct Mol Biol 2009;16:987-9.
25. Han D, Kim K, Kim Y, Kang Y, Lee JY, Kim Y. Crystal structure of the N-terminal domain of anaphase-promoting complex subunit 7. J Biol Chem 2009;284:15137-46.
26. Pal M, Nagy O, Menesi D, Udvardy A, Deak P. Structurally related TPR subunits contribute differently to the function of the

anaphase-promoting complex in Drosophila melanogaster. J Cell Sci 2007;120:3238-48.
27. Lamb JR, Michaud WA, Sikorski RS, Hieter PA. Cdc16p, Cdc23p AND Cdc27p form a complex essential for mitosis. EMBO J 1994;13:4321-8.
28. Bolanos-Garcia VM. The N-terminal, TPR-containing domain of the mitotic checkpoint protein BUBR1 does not bind fatty acids. Comput Biol Chem 2008;32:139-40.
29. Millson SH, Vaughan CK, Zhai C, Ali MM, Panaretou B, Piper PW, *et al.* Chaperone ligand-discrimination by the TPR-domain protein Tah1. Biochem J 2008;413:261-8.
30. Lapouge K, Smith SJ, Walker PA, Gamblin SJ, Smerdon SJ, Rittinger K. Structure of the TPR domain of p67phox in complex with Rac.GTP. Mol Cell 2000;6:899-907.
31. Taylor P, Dornan J, Carrello A, Minchin RF, Ratajczak T, Walkinshaw MD. Two structures of cyclophilin 40: Folding and fidelity in the TPR domains. Structure 2001;9:431-8.
32. Blatch GL, Lassle M. The tetratricopeptide repeat: A structural motif mediating protein-protein interactions. Bioessays 1999;21:932-9.
33. D'Andrea LD, Regan L. TPR proteins: The versatile helix. Trends Biochem Sci 2003;28:655-62.
34. Vodermaier HC, Gieffers C, Maurer-Stroh S, Eisenhaber F, Peters JM. TPR subunits of the anaphase-promoting complex mediate binding to the activator protein CDH1. Curr Biol 2003;13:1459-68.
35. Singh N, Wiltshire TD, Thompson JR, Mer G, Couch FJ. Molecular basis for the association of microcephalin (MCPH 1) protein with the cell division cycle protein 27 (Cdc27) subunit of the anaphase-promoting complex. J Biol Chem 2012;287:2854-62.
36. Zeng X, Sigoillot F, Gaur S, Choi S, Pfaff KL, Oh DC, *et al.* Pharmacologic inhibition of the anaphase-promoting complex induces a spindle checkpoint-dependent mitotic arrest in the absence of spindle damage. Cancer Cell 2010;18:382-95.
37. UniProt Consortium. The Universal Protein Resource (UniProt) 2009. Nucleic Acids Res 2009;37:D169-74.
38. Larkin MA, Blackshields G, Brown NP, Chenna R, McGettigan PA, McWilliam H, *et al.* Clustal W and Clustal X version 2.0. Bioinformatics 2007;23:2947-8.
39. Waterhouse AM, Procter JB, Martin DM, Clamp M, Barton GJ. Jalview Version 2: A multiple sequence alignment editor and analysis workbench. Bioinformatics 2009;25:1189-91.
40. Cole C, Barber JD, Barton GJ. The Jpred 3 secondary structure prediction server. Nucleic Acids Res 2008;36:W197-201.
41. Eswar N, Webb B, Marti-Renom MA, Madhusudhan MS, Eramian D, Shen MY, *et al.* Comparative protein structure modeling using modeller. Curr Protoc Bioinformatics 2006;Chapter 5:Unit 5.6.
42. Söding J, Biegert A, Lupas AN. The HHpred interactive server for protein homology detection and structure prediction. Nucleic Acids Res 2005;33:W244-8.
43. Van Der Spoel D, Lindahl E, Hess B, Groenhof G, Mark AE, Berendsen HJ. GROMACS: Fast, flexible, and free. J Comput Chem 2005;26:1701-18.
44. Lindorff-Larsen K, Piana S, Palmo K, Maragakis P, Klepeis JL, Dror RO, *et al.* Improved side-chain torsion potentials for the Amber ff99SB protein force field. Proteins 2010;78:1950-8.
45. Jorgensen WL, Chandrasekhar J, Madura JD, Impey RW, Klein ML. Comparison of simple potential functions for simulating liquid water. J Chem Phys 1983;79:926-35.
46. Hess B, Bekker H, Berendsen HJ, Fraaije JG. LINCS: A linear constraint solver for molecular simulations. J Comput Chem 1997;18:1463-72.
47. Berendsen HJ, Postma JP, Van der Gunsteren WF, Dinola A, Haak JR. Molecular dynamics with coupling to an external bath. J Chem Phys 1984;81:3684-90.
48. Parrinello M, Rahman A. Crystal structure and pair potentials: Molecular dynamics study. Phys Rev Lett 1980;45:1196-9.
49. Merlino A, Mazzarella L, Carannante A, Di Fiore A, Donato A, Notomista E, *et al.* The importance of dynamic effects on the enzyme activity: X-ray structure and molecular dynamics of onconase mutants. J Biol Chem 2005;280:17953-60.
50. Laskowski RA, MacArthur MW, Moss DS, Thornton JM. PROCHECK: A program to check the stereochemical quality of protein structures. J Appl Crystallogr 1993;26:283-91.
51. Luthy R, Bowie JU, Eisenberg D. Assessment of protein models with three-dimensional profiles. Nature 1992;356:83-5.
52. Morris GM, Huey R, Lindstrom W, Sanner MF, Belew RK, Goodsell DS, *et al.* AutoDock4 and AutoDockTools4: Automated docking with selective receptor flexibility. J Comput Chem 2009;30:2785-91.
53. Laskowski RA, Swindells MB. LigPlot+: Multiple ligand-protein interaction diagrams for drug discovery. J Chem Inf Model 2011;51:2778-86.
54. Jackson PK, Eldridge AG, Freed E, Furstenthal L, Hsu JY, Kaiser BK, *et al.* The lore of the RINGs: Substrate recognition and catalysis by ubiquitin ligases. Trends Cell Biol 2000;10:429-39.
55. Brinker A, Scheufler C, Von Der Mulbe F, Fleckenstein B, Herrmann C, Jung G, *et al.* Ligand discrimination by TPR domains. Relevance and selectivity of EEVD-recognition in Hsp70×Hop×Hsp90 complexes. J Biol Chem 2002;277:19265-75.
56. Kobayashi K, Sueyoshi T, Inoue K, Moore R, Negishi M. Cytoplasmic accumulation of the nuclear receptor CAR by a tetratricopeptide repeat protein in HepG2 cells. Mol Pharmacol 2003;64:1069-75.
57. Magliery TJ, Regan L. Beyond consensus: Statistical free energies reveal hidden interactions in the design of a TPR motif. J Mol Biol 2004;343:731-45.
58. Carrigan PE, Nelson GM, Roberts PJ, Stoffer J, Riggs DL, Smith DF. Multiple domains of the co-chaperone Hop are important for Hsp70 binding. J Biol Chem 2004;279:16185-93.
59. Das AK, Cohen PW, Barford D. The structure of the tetratricopeptide repeats of protein phosphatase 5: Implications for TPR-mediated protein-protein interactions. EMBO J 1998;17:1192-9.
60. Buschhorn BA, Petzold G, Galova M, Dube P, Kraft C, Herzog F, *et al.* Substrate binding on the APC/C occurs between the coactivator Cdh1 and the processivity factor Doc1. Nat Struct Mol Biol 2011;18:6-13.
61. da Fonseca PC, Kong EH, Zhang Z, Schreiber A, Williams MA, Morris EP, *et al.* Structures of APC/CCdh1 with substrates identify Cdh1 and Apc10 as the D-box co-receptor. Nature 2011;470:274-8.
62. Vodermaier H, Gieffers C, Maurer-Stroh S, Eisenhaber F, Peters JM, Gmachl M, inventors. Method of identifying compounds that specifically inhibit the anaphase promoting complex; 2005.
63. Cliff MJ, Williams MA, Brooke-Smith J, Barford D, Ladbury JE. Molecular recognition via coupled folding and binding in a TPR domain. J Mol Biol 2005;346:717-32.

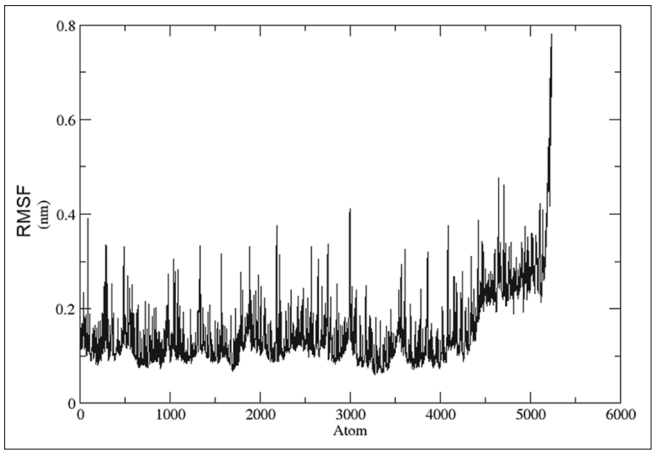

Supplementary Figure 1: RMSF (root mean square fluctuation) showed that the APC3 structure model is stable during MD, only the last TPR domain has more flexibility